JOURNAL OF GEOPHYSICAL RESEARCH, VOL. 103, NO. D9, PAGES 10,593–10,604, MAY 20, 1998

# Studying the effects of aerosols on vertical photolysis rate coefficient and temperature profiles over an urban airshed

Mark Z. Jacobson
Department of Civil and Environmental Engineering, Stanford University, Stanford, California

**Abstract.** This paper discusses the effects of size- and composition-resolved aerosols on photolysis and temperatures within and above an urban airshed. With respect to photolysis, three-dimensional simulations indicated that (1) in regions of the boundary layer where absorption of ultraviolet (UV) radiation was strong, aerosols reduced photolysis coefficients of UV-absorbing gases; (2) in regions of the boundary layer where UV scattering dominated UV absorption by aerosols, aerosols enhanced photolysis coefficients of UV-absorbing gases; (3) aerosols increased photolysis coefficients for visible-absorbing gases since visible scattering always exceeded visible absorption by aerosols; (4) scattering and weakly absorbing aerosols above the boundary layer increased photolysis coefficients above the boundary layer for all absorbing gases; and (5) increases in aerosol absorption extinction within the boundary layer reduced photolysis coefficients above the boundary layer for all absorbing gases. Photolysis coefficients changes due to aerosols decreased near-surface ozone mixing ratios in Los Angeles by 5-8%. With respect to temperatures, simulations indicated that aerosols increased radiative heating rates at all altitudes but decreased surface solar irradiances during the day. Surface irradiance reductions cooled the ground, reducing mechanical and thermal turbulent heat fluxes back to the boundary layer, cooling near-surface air, and stabilizing the boundary layer. During the night, aerosols decreased boundary-layer heating rates but increased downward infrared irradiances to the ground. Warmer ground temperatures increased mechanical turbulent heat fluxes to the boundary layer, increasing nighttime near-surface temperatures. Thus, aerosols affected temperatures primarily through ground-atmosphere turbulent heat transfer.

## 1. Introduction

This paper presents the first three-dimensional modeling study of the effects of size- and composition-resolved aerosols on vertical profiles of temperatures, ultraviolet irradiances, and photolysis rate coefficients over an urban airshed. One-dimensional studies of the effects of boundary-layer pollution on solar fluxes, radiative heating rates, and/or temperatures have been carried out by *Myrup* [1969], *Atwater* [1971a, b], *Zdunkowski and McQuage* [1972], *Bergstrom and Viskanta* [1973], *Bergstrom* [1973 a, b], *Zdunkowski et al.* [1976], *Welch and Zdunkowski* [1976], Ackerman [1977], *Estournel et al.* [1983], *Tanaka* [1990], *Kilsby* [1990], and *Wendisch et al.* [1996], among others. One-dimensional studies of ultraviolet (UV) irradiances, actinic fluxes, and/or $NO_2$ photolysis coefficients in a polluted or cloudy atmosphere have been done by *Madronich* [1987], *van Weele and Duynkerke* [1993], *de Arellano et al.* [1994], *Ruggaber et al.* [1994], *Forster* [1995], and *Wendisch et al.* [1996], among others. A three-dimensional study of the effects of a horizontally-uniform but spectrally-varying aerosol optical depth on photolysis and ozone has been carried out by *Dickerson et al.* [1997].

Aerosols affect photolysis rate coefficients and temperatures. Both parameters affect ozone and other trace gas mixing ratios. Temperatures affect air pressures and wind speeds. Aerosols affect temperatures in at least three ways. They backscatter a fraction of incoming solar radiation, thereby increasing the earth-atmosphere albedo and lowering surface air temperatures during the day. Some aerosols absorb solar radiation and emit infrared radiation, decreasing the cooling effect of backscattering. Most aerosols also absorb and emit infrared radiation, decreasing the cooling effect caused by backscattering during the day and increasing air temperatures at night [e.g., *Rasool and Schneider*, 1971; *Zdunkowski and McQuage*, 1972; *Chylek and Coakley*, 1974; *Weare et al.*, 1974; *Zdunkowski et al.*, 1976].

In an early study of the effects of aerosols on urban temperatures, *Zdunkowski and McQuage* [1972] used a one-dimensional aerosol-radiative model to find that aerosols caused a net warming of urban surface air over a short period of time (e.g., 1 day), but a net cooling thereafter. Because of computer limitations, the study neglected infrared scattering, solar effects on atmospheric heating, wavelength dependence of radiative transfer, and detailed treatment of soil processes, resulting in large surface temperature swings from aerosols of 2-4 K per day. A three-dimensional study by *Jacobson* [1997b] supported part of their hypothesis by showing that aerosols in the Los Angeles basin caused surface air temperatures to cool during the day and warm to a greater extent at night, yielding a net warming, averaged over day and night. The net warming was maintained for the length of the simulation period, which was 2 days. The swings in temperature due to aerosols in this study were 0.2-0.8 K.

In a study of the effects of aerosols on UV irradiance and photolysis coefficients, *Wendisch et al.* [1996] compared radiative predictions from a one-dimensional model to data to show that an enhanced aerosol layer within a temperature



Paper number 98JD00287
0148-0227/98/98JD-00287$09.00

inversion reduced downwelling solar and UV irradiances and $NO_2$ photolysis rate coefficients in comparison with a background aerosol layer.

In studies of the effects of clouds on actinic flux and photolysis, *Madronich* [1987], *van Weele and Duynkerke* [1993], and *de Arellano et al.* [1994] showed that clouds increase the backscattered fraction of incident solar radiation, enhancing actinic fluxes above them. They also showed that clouds increase actinic fluxes within cloud layers and decrease actinic fluxes below cloud layers. Because of their high albedos, low clouds tend to reduce downward irradiance and temperatures below them. Because of their relatively low albedos but strong absorptivity, high clouds tend to increase temperatures below them [e.g., *Liou*, 1992].

A study of the effects of aerosols on temperatures and photolysis in three dimensions is important for two reasons. First, the effects of aerosols on near-surface temperatures depend strongly on turbulent fluxes between the ground surface and the boundary layer. Such fluxes are best calculated from three-dimensional wind fields together with a turbulence parameterization when detailed observations are not available. Second, an important aspect of the effects of aerosols on photolysis is the effect of photolysis changes on ozone. Since the simulation of ozone in an urban airshed requires calculations of emissions, chemistry, and transport over a three-dimensional grid, a study of the effects of aerosols on photolysis and ozone is inherently a three-dimensional problem.

## 2. Description of the Model

The model to be used for this study is GATORM, a gas, aerosol, transport, radiation, and meteorological model [*Jacobson*, 1994; 1997a,b; *Jacobson et al.*, 1996a] The meteorological component was developed by *Lu and Turco* [1995]. GATORM is the first three-dimensional model in which gas, size-resolved aerosol, radiative, and meteorological parameters have been compared simultaneously to data from a comprehensive database [*Jacobson*, 1994; 1997b] and the first gas / size-resolved aerosol air quality model to feed radiative heating rates back to a meteorological module for temperature calculations. Figure 1 shows a diagram of the processes simulated in the model.

GATORM solves the continuity equations for air, trace gases, aerosol number concentration, and aerosol volume concentration. It also solves the thermodynamic energy equation, the horizontal momentum equations, the equation for geopotential, and a spectral form of the radiative transfer equation. Gases are affected by emissions, chemistry, dry deposition, gas-to-particle conversion, and transport. Chemistry is solved with a sparse-matrix, vectorized Gear-type ordinary differential equation solver, SMVGEAR II [*Jacobson*, 1995, 1998a].

Size-resolved aerosols in the model are affected by emissions, nucleation, coagulation, growth, internal reversible reactions, internal irreversible reactions, sedimentation, dry deposition, and transport. Homogeneous nucleation of sulfuric acid-water is treated empirically. Coagulation is solved with a semi-implicit scheme [*Jacobson et al.*, 1994]. Gas-aerosol transfer of $H_2O$, $H_2SO_4$, other condensible inorganics, and condensible organics is treated with an unconditionally stable numerical scheme [Jacobson, 1997c]. Transfer of $HNO_3$, $NH_3$, HCl, other soluble inorganics, and soluble organics is also treated with an unconditionally stable scheme [Jacobson, 1997c]. Internal

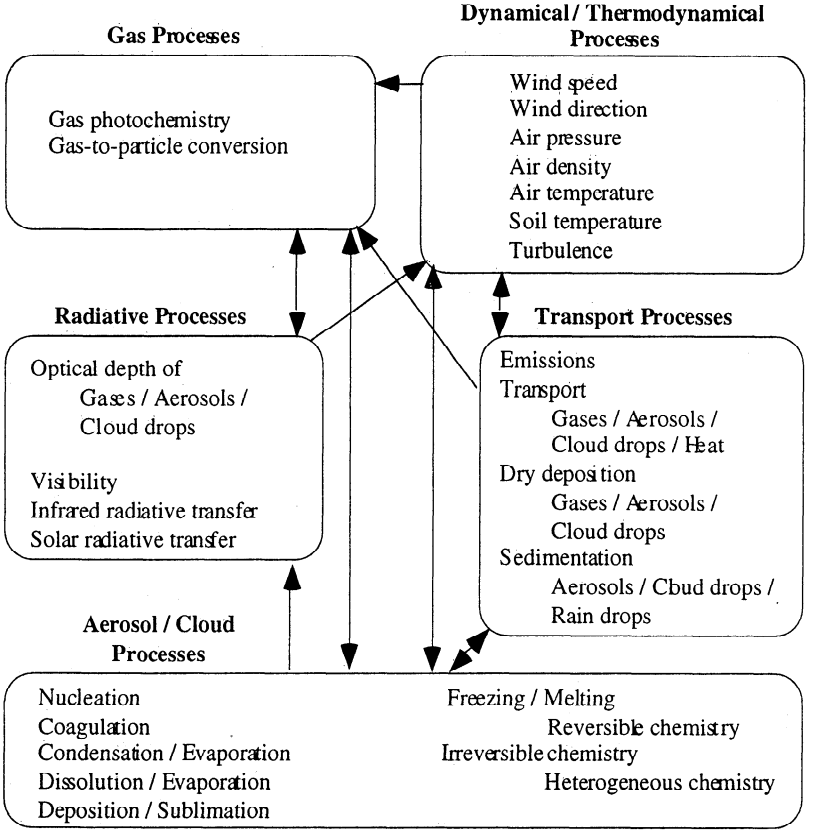


**Figure 1.** Diagram of processes simulated in GATORM and the interactions among them.

aerosol composition, including liquid water content (micrograms of liquid water per cubic meter of air) resulting from hydration of water with solute, is determined with a chemical equilibrium code, EQUISOLV [*Jacobson et al.*, 1996b]. Aerosols in the model can grow to cloud-sized drops, in which case their liquid water contents increase significantly. Irreversible aqueous reactions, which are important in cloud drops, are simulated with SMVGEAR II.

The model uses 16 size bins geometrically spaced from 0.014- to 74-μm diameter, with a volume ratio between adjacent size bins of 5. All particles in a size bin are assumed to have identical composition. During growth, particles sizes increase or decrease and are allowed to cross size bin diameter boundaries. If particles grow larger than the high edge diameter of their size bin, all particles in the bin are moved to the size bin bounding their average diameter. Size bin boundaries are maintained for emissions, nucleation, coagulation, and transport. This size structure, called the moving-center structure [Jacobson, 1997a], reduces numerical diffusion during growth.

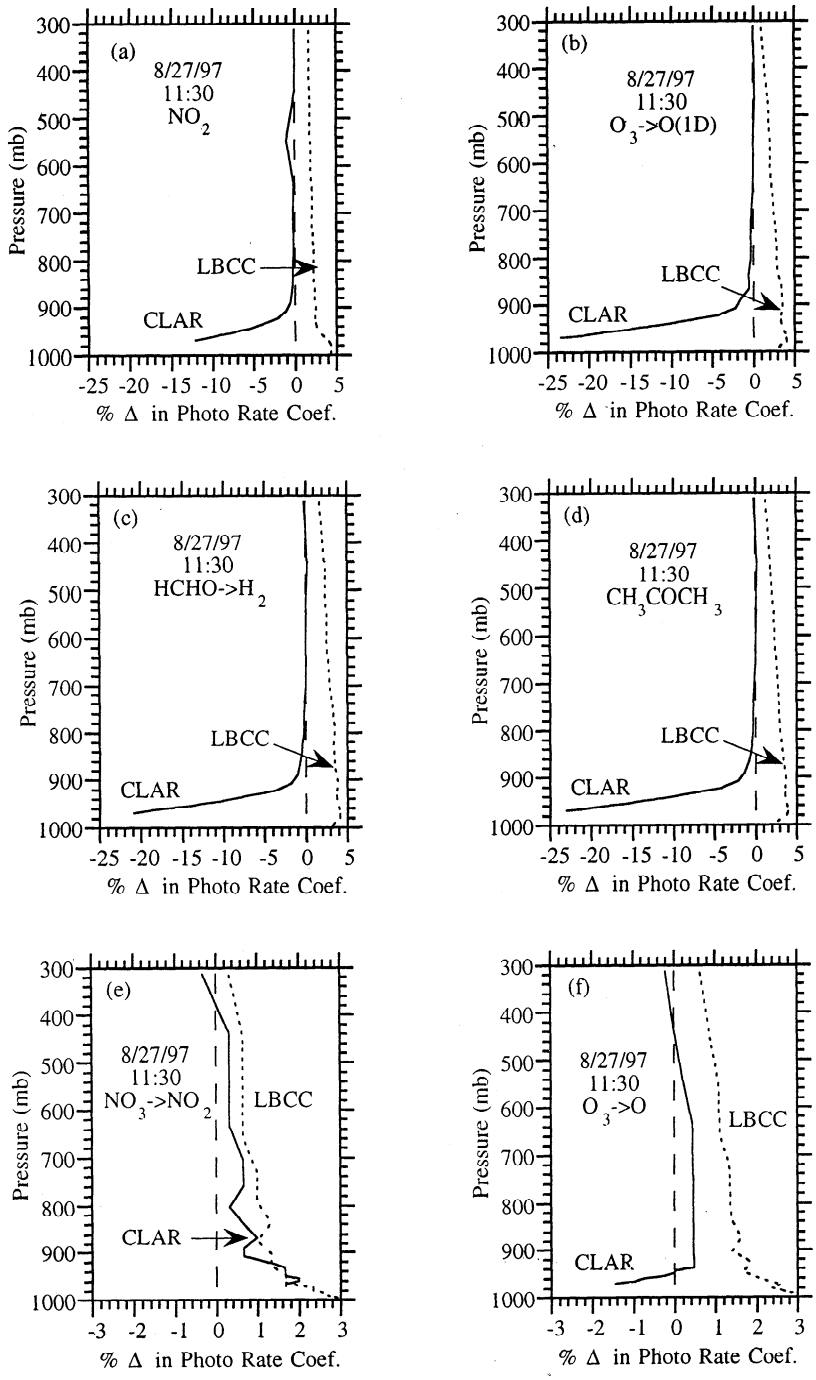


**Figure 2.** Percent difference between photolysis rate coefficients from the baseline simulation and the gas-only simulation for several photoprocesses at Claremont (CLAR) and Long Beach City College (LBCC). A positive value indicates that aerosols enhanced photolysis rate coefficients. The vertical line at 0 is for reference.

For tropospheric calculations, photolysis coefficients in the model are determined for 67 UV and visible wavelength intervals between 0.285 and 0.8 μm. Most intervals appear below 0.43 μm. Photolysis coefficients depend on spectral actinic fluxes, absorption cross-section data, and quantum yield data, all averaged over each wavelength interval. Spectral actinic fluxes, which are found by integrating spectral radiances over all solid angles of a sphere, are calculated for each wavelength with a tridiagonal matrix solution to the radiative transfer equation [*Toon et al.*, 1989]. The equation is solved for each grid cell in each column, assuming no interactions between columns. The solution assumes that the scattering phase function integrals for diffuse radiation can be approximated with a two-point quadrature equation [*Liou*, 1974]. Extinction coefficients are affected by gas (Rayleigh) scattering, gas absorption, particle scattering, and particle absorption. Current mixing ratios of ozone, oxygen, and all other photodissociating gases affect extinction due to gas absorption. Particles accounted for in extinction calculations include aerosols, liquid cloud drops, and ice crystals. Scattering, absorption, and forward scattering efficiencies for a given particle size, wavelength, core index of refraction, and shell index of refraction are calculated with a Mie code for stratified spheres [*Toon and Ackerman*, 1981].

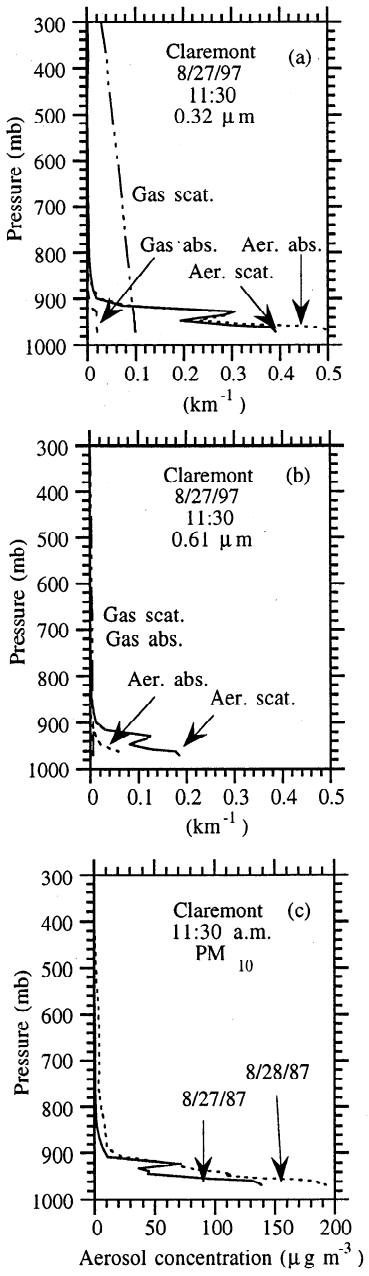


**Figure 3.** Predicted vertical profiles from Claremont of extinction coefficients (km$^{-1}$) due to gas scattering, aerosol scattering, gas absorption, and aerosol absorption at band centered at (a) 0.32 and (b) 0.61 μm (band boundaries are 0.3175-0.3225 and 0.605-0.615 μm, respectively) for the baseline simulation. (c) Predicted vertical profile of mass concentration in particles smaller than 10 μm in diameter at 1130 on August 27 and 28, 1987. All figures indicate the presence of elevated aerosol layers.

Heating rates from the radiative transfer module drive part of the diabatic temperature change in the thermodynamic energy equation of the meteorological module. In *Jacobson* [1997b], this method resulted in predicted near-surface temperatures errors, averaged over all monitoring stations and times, of less than 1.9 K. Heating rates are calculated from irradiances, determined with the two-stream solver for 67 wavelength intervals smaller than 0.8 μm, 67 intervals between 0.8 and 4.5 μm, and 88 intervals between 4.5 and 1000 μm. Absorption extinction coefficients in the near and far infrared are determined from absorption coefficients, weighted over probability intervals. Gases in the model that absorb far-infrared radiation include $H_2O$, $CO_2$, $O_3$, $CH_4$, $N_2O$, $CFCl_3$, $CF_2Cl_2$, $CFCl_3$, and $CCl_4$. Far-infrared absorption coefficient data were obtained from *Mlawer et al.* [1997].

## 3. Optical Properties of Los Angeles Aerosols

Accurate predictions of spectral actinic flux and irradiance depend largely on predictions of aerosol size distributions, compositions, absorption efficiencies, scattering efficiencies, and forward scattering efficiencies. The model described above predicts aerosol composition and size, including aerosol liquid water content. *Jacobson* [1997a, b] calculated absorption, scattering, and forward scattering efficiencies with the Mie algorithm described above by assuming that core material was elemental carbon. Effective real and imaginary indices of refraction of shell material were calculated by averaging individual indices, by volume, over all shell components. Such a method worked for obtaining optical properties in the visible spectrum but was found recently to be insufficient for predicting optical properties of Los Angeles aerosols in the UV spectrum.

Data from the Southern California Air Quality Study period of August 26-29, 1987 indicated that peak downwelling direct plus diffuse surface UV irradiances (0.295-0.385 μm) measured at central Los Angeles (elevation of 87 m), Claremont (elevation of 364 m), and Riverside (elevation of 249 m) were about 22%, 33%, and 46% less, respectively, than those measured at Mount Wilson (elevation of 1739 m). Simulations of these reductions indicated that aerosol scattering, elemental carbon absorption, and gas absorption, together, could not account for observed UV reductions. Absorption by ozone and other UV-absorbing gases was not nearly sufficient to obtain observed decreases in UV irradiance. Elemental carbon, regardless of whether it was treated as a core surrounded by a shell, as a shell, or as a core with no shell, also did not absorb sufficiently. Varying the peak radius or vertical profiles of

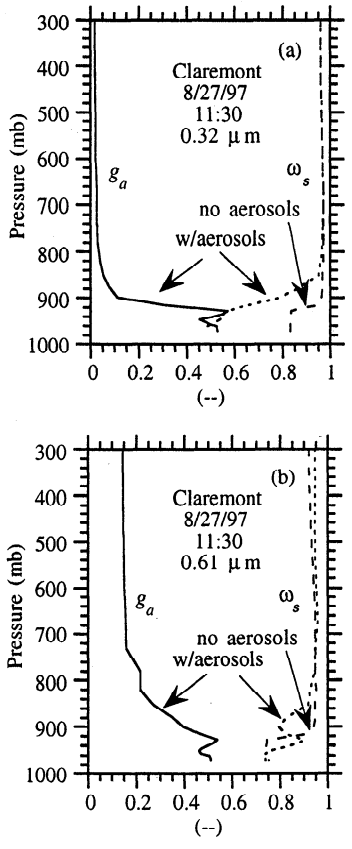


**Figure 4.** Vertical profiles from Claremont of the overall asymmetry factor and single-scattering albedo at (a) 0.32 and (b) 0.61 μm for the baseline (with aerosols) and gas-only (no aerosols) simulations. The overall asymmetry factor was zero at all altitudes for the gas-only simulation. Band boundaries are the same as for Figure 3.

particles did not improve matters. Soil particles, whose imaginary index of refraction increases from the visible to UV spectra, did not absorb sufficiently either. Together, the processes above accounted for less than an 13% UV reduction at Claremont and a 23.5% UV reduction at Riverside.

It was hypothesized that the cause of remaining UV reductions was UV absorption by certain organic and nitrated inorganic compounds present within particles [M. Z. Jacobson, Uncovering the role of organic aerosols on ultraviolet light absorption in the atmosphere, in preparation]. These compounds included nitrated aromatics, benzaldehydes, other aldehydes, benzoic acids, aromatic polycarboxylic acids, phenols, polycyclic aromatic hydrocarbons, certain organic bases, and ammonium nitrate. Many such compounds have peak absorption wavelengths between 0.27 and 0.4 μm.

With this information, GATORM was modified to account for UV absorption by organics and nitrated inorganics. Because imaginary index of refraction data are unavailable for almost all organics, index of refraction data for liquid nitrobenzene, obtained from *Foster* [1992], were used as a surrogate in model simulations. Ammonium nitrate, sodium nitrate, and the nitrate ion were assumed to have UV imaginary indices of refraction for ammonium nitrate, which was derived from data reported in the literature [M. Z. Jacobson, Uncovering the role of organic aerosols on ultraviolet light absorption in the atmosphere, in preparation]. The model was further modified to treat secondary organics as shell material and the rest of each particle as core material when particles contained more than 5% secondary organic material and UV wavelengths were considered. For visible wavelengths and when particles contained less than 5% secondary carbon, the secondary carbon shell was assumed to be relatively transparent. In such cases, elemental carbon was assumed to be core material, and all other material was assumed to be shell

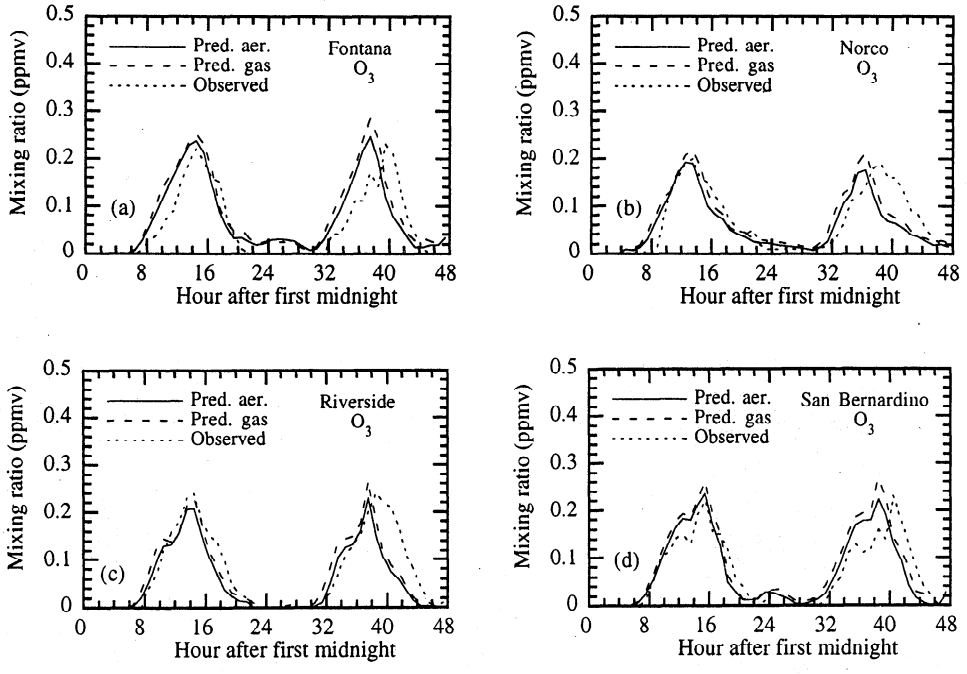


**Figure 5.** Comparison of near-surface ozone predicted when aerosols and UV absorption by organics and nitrated inorganics were accounted for ("pred. aer."), predicted when aerosols were excluded ("pred. gas"), and observed on August 27 - 28, 1987.

material. Secondary organic condensation was accounted for by assuming that a fraction of certain organic gases, such as benzaldehyde, peroxybenzoyl nitrate, cresol, and nitrophenol, among others, could convert to condensable products. The fractions were obtained from aerosol yields of *Pandis and Seinfeld* [1992]. Those yields gave the mass concentration of aerosol formed per unit emissions of an organic precursor. Instead of applying the yields to emissions, the yields were applied to gases as they were formed chemically, which allowed certain emitted organics to react in the gas phase before its products were converted to the particle phase.

## 4. Description of the Simulations

For this study, simulations with GATORM were carried out over the Los Angeles basin for August 27-28, 1987 to estimate the effects of aerosols on photolysis, ozone, and heating rates. The model grid southwest corner was located at 32.97°N latitude and 119.25°W longitude. The horizontal spherical coordinate grid included 66 west-east grid cells by 42 south-north cells. Grid spacing was 0.05° west-east (about 4.6 km) and 0.045° south-north (about 5.0 km). In the vertical, 20 sigma-pressure coordinate layers between the topographical surface and 250 mbar were used for all calculations. Approximately eight layers resided below 850-mbar (1.5 km) altitude.

The model treated 111 gases and 36 aerosol components in each of the 16 size bins. The gas- and aqueous-phase chemical mechanisms used for this study are given by *Jacobson* [1998b]. Original gas and aerosol emissions rates for this study are described by *Jacobson et al.* [1996] and *Jacobson* [1997b], respectively. The original aerosol inventory has been modified downward several times by the *South Coast Air Quality Management District* [1996] so that it is now about 33% of its original value. Sensitivity tests of *Jacobson* [1997b] indicated that cutting the entire inventory to 33% of their initial value increased underpredictions of some species without improving gross errors. For this study, emissions rates of all species, except for sulfates and organic carbon, were reduced to 40% of their original values. Emissions rates of sulfates and organic carbon were reduced to 70% of their original values.

Two simulations were run. The first, called the baseline simulation, included all model processes. The second, called the gas-only simulation, included all processes except aerosol processes. Aerosols, themselves, were absent during the gas-only simulation. The baseline and gas-only simulations were compared with each other and with surface and upper air data, where possible. Results are discussed below.

## 5. Effects of Aerosols on Photolysis Coefficients

Figures 2a-2f shows differences between photolysis coefficient profiles from the baseline and gas-only simulations at 1130 a.m. on August 27, 1987 at Claremont and Long Beach City College. The first four panels (Figures 2a-2d) show differences for gases that photolyze in the UV spectrum. At Claremont, boundary layer photolysis coefficients for UV-absorbing gases decreased when aerosols were accounted for. Figure 3a shows that, in the boundary layer at Claremont, UV absorption extinction coefficients exceeded UV scattering coefficients. Strong aerosol absorption caused the reductions in UV actinic fluxes and corresponding photolysis coefficients that are seen in Figures 2a-2d.

A reduced presence of UV-absorbing aerosols at Long Beach enhanced photolysis coefficients there. UV photolysis coefficients in the boundary layer at Long Beach were enhanced because UV scattering dominated UV absorption at Long Beach. Scattering aerosols enhance actinic fluxes and, therefore, photolysis coefficients by increasing backscattered radiation. Since actinic fluxes depend on radiation from all solid angles of a sphere, increases in backscattered radiation increase actinic fluxes in the absence of absorption. At Claremont, absorption by aerosols decreased backscattered and ground-reflected radiation, decreasing actinic fluxes and photolysis coefficient enhancements caused by backscattering.

Figures 2e-2f show photolysis profile differences for gases that photolyze in the visible or visible / UV spectra. In the visible spectrum, extinction due to aerosol scattering exceeded extinction due to aerosol absorption at Claremont, as is shown in Figure 3b. These conditions caused photolysis coefficients for the visible wavelength photoprocess, $NO_3 \rightarrow NO_2$, to increase at Claremont, as is shown in Figure 2e. Enhancement occurred because scattering aerosols increased backscattered radiation in the visible spectrum at Claremont.

The photoprocess $O_3 \rightarrow O(^3P)$ occurs in the ultraviolet and visible spectra. Figure 2f shows that aerosols caused photolysis coefficients for this process to decrease at Claremont and increase at Long Beach in the boundary layer. Thus, aerosol absorption extinction coefficients were greater at Claremont than at Long Beach for wavelengths affecting $O_3 \rightarrow O(^3P)$ photolysis.

Figures 2a-2f indicate that the presence of scattering aerosols within and above the boundary layer enhanced photolysis coefficients above the boundary layer at Long Beach. Such enhancements would also have occurred at Claremont, except that strong boundary layer absorption at Claremont reduced the effects of backscattering above the boundary layer.

Figure 3c shows predicted vertical profiles of total <10 μm aerosol mass concentration (dry mass plus liquid water) at Claremont at 1130 on August 27 and 28, 1987. The figure shows an elevated aerosol layer on August 27 that merges with the surface aerosol layer on August 28. The elevated layer appears on the extinction coefficient diagrams in Figures 3a-3b as well. *Wakimoto and McElroy* [1986] observed weak elevated aerosol layers above Claremont.

Figures 4a-4b show predicted overall asymmetry factors and single-scattering albedos for the baseline and gas-only simulations at Claremont. The overall asymmetry factor and the single-scattering albedo at each wavelength are

$$g_a = \frac{\sigma_{s,p} g_{a,p} + \sigma_{s,c} g_{a,c}}{\sigma_{s,g} + \sigma_{s,p} + \sigma_{s,c}} \quad (1)$$

$$\omega_s = \frac{\sigma_{s,g} + \sigma_{s,p} + \sigma_{s,c}}{\sigma_{s,g} + \sigma_{s,p} + \sigma_{s,c} + \sigma_{a,g} + \sigma_{a,p} + \sigma_{a,c}} \quad (2)$$

respectively, where $g_{a,p}$ is the asymmetry parameter for particles aside from cloud drops, $g_{a,c}$ is the asymmetry parameter for cloud drops, $\sigma_{s,g}$ is the extinction coefficient ($m^{-1}$) due to gas scattering, $\sigma_{s,p}$ is the extinction coefficient due to noncloud particle scattering, $\sigma_{s,c}$ is the extinction

coefficient due to cloud scattering, $\sigma_{a,g}$ is the extinction coefficient due to gas absorption, $\sigma_{a,p}$ is the extinction coefficient due to noncloud particle absorption, and $\sigma_{a,c}$ is the extinction coefficient due to cloud absorption.

Since the asymmetry parameter for Rayleigh scattering is zero, it does not appear in (1). The overall asymmetry parameters above the boundary layer in Figures 4a-4b are smaller than single-particle asymmetry parameters because Rayleigh scattering dominated scattering extinction above the boundary layer at all wavelengths, as is partly seen in Figures 3a-3b. Since extinction due to Rayleigh scattering dominated above the boundary layer, overall asymmetry parameters above the boundary layer in Figures 4a-4b were relatively low. Within the boundary layer, overall asymmetry parameters increased because aerosol scattering extinction dominated Rayleigh scattering extinction, as is indicated in Figures 3a-3b.

The single-scattering albedo is the ratio of extinction due to scattering to total extinction. The single-scattering albedo curves in Figures 4a-4b indicate that, above the boundary layer, ultraviolet extinction was due almost entirely to gas scattering in the gas-only simulation and gas/particle scattering in the baseline simulation. Absorption played a larger role within the boundary layer than above the boundary layer. In the gas-only simulation, about 15-30% of extinction in the boundary layer at all wavelengths was due to gas

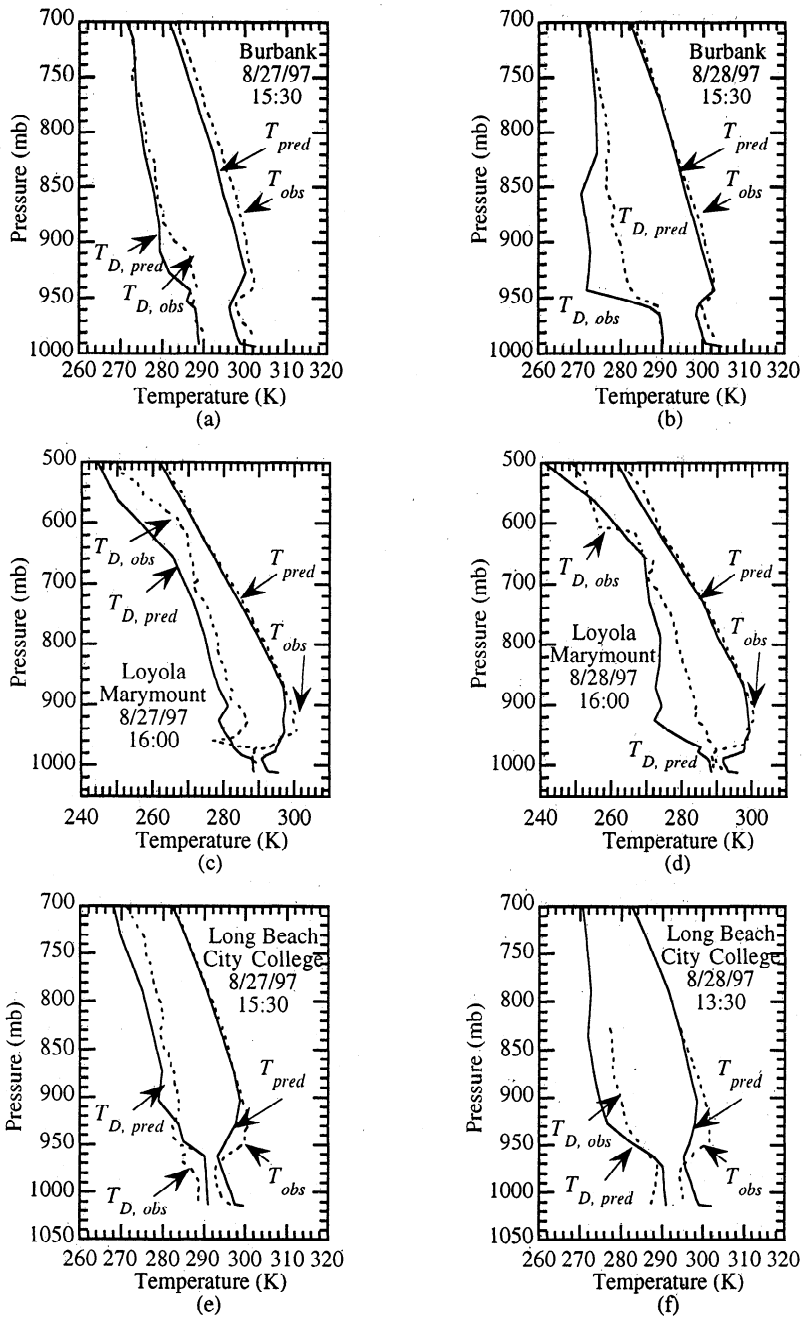


**Figure 6.** Comparison of predicted (baseline simulation) and observed vertical profiles of temperature and dew point temperature at several locations in the Los Angeles basin on the afternoons of August 27 and 28 or evening of August 28, 1987. Predicted temperature profiles include ground surface temperature. Observations did not include ground surface temperatures.

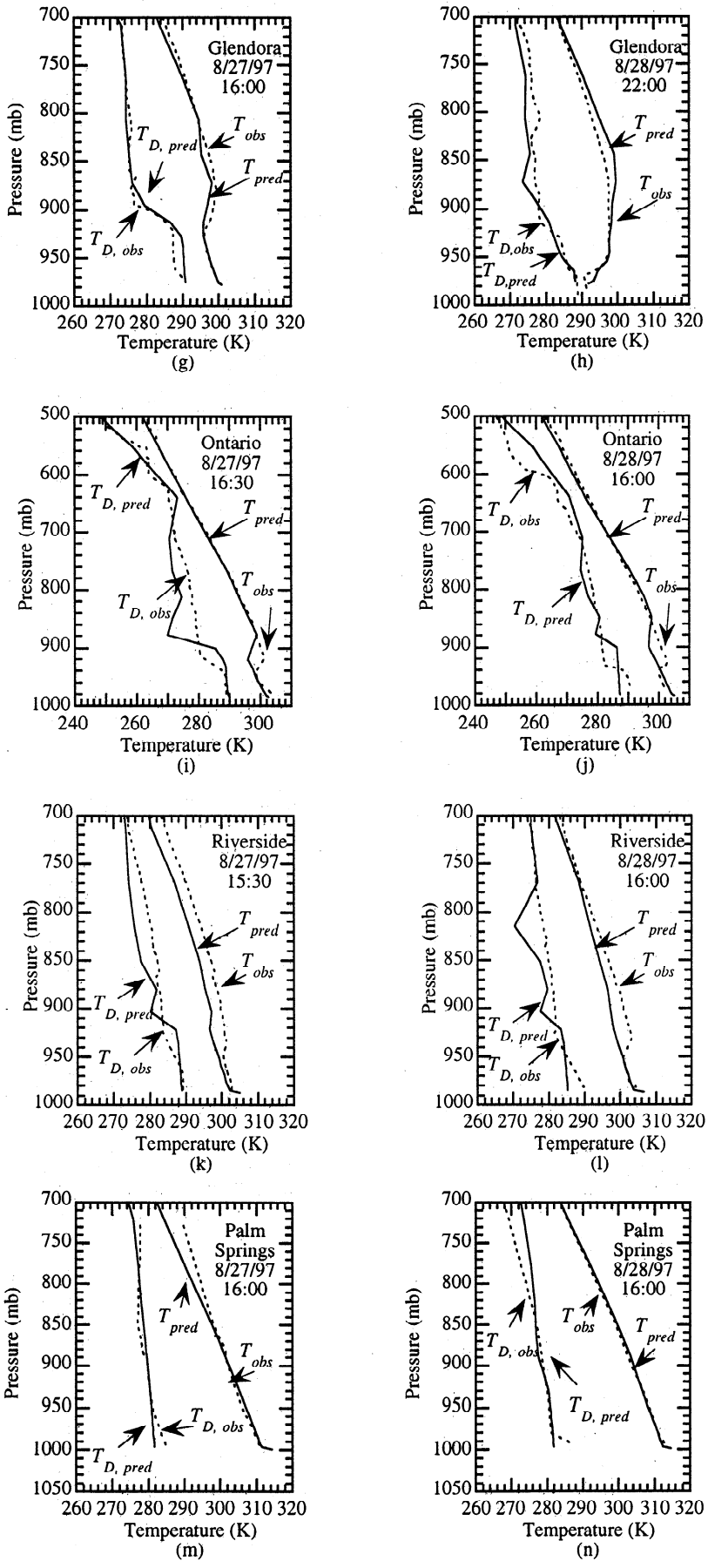


**Figure 6.** (continued)

absorption, and the rest was due to Rayleigh scattering. The addition of aerosols reduced the single-scattering albedo more in the UV spectrum than in the visible spectrum because extinction coefficients due to aerosol absorption increased from the UV spectrum to the visible spectrum, as is shown in Figures 3a-3b.

## 6. Effects of Aerosols on Near-Surface Ozone

Changes in photolysis rate coefficients affect mixing ratios of ozone and other gases. Aerosols affect ozone mixing ratios in at least three ways. First, they alter air temperature, which affects chemical reaction rate coefficients, atmospheric stability, air pressure, velocities, and, therefore, ozone. Second, organic gas precursors of ozone may also condense upon, dissolve within, or react on aerosol surfaces. NO, $NO_2$, and $O_3$ do not noticeably dissolve within or condense upon aerosols. These gases may react on aerosol surfaces, but their rates of reaction on urban aerosols have not been verified. Third, aerosols affect ozone by altering photolysis coefficients. *Jacobson* [1997b] used a three-dimensional model to estimate that the presence of aerosols caused a 2% decrease in near-surface ozone mixing ratios throughout the Los Angeles basin during a 2-day period. The value was obtained by comparing baseline simulation ozone predictions, averaged over all Southern California Air Quality Study surface sites and hours of simulation, to averaged gas-only simulation predictions.

The treatment of ultraviolet aerosol absorption and secondary organic aerosol growth is more rigorous in this study than in the previous study, and aerosols were found here to decrease near-surface ozone mixing ratios by 5-8%. Most of the reductions in ozone were due to reductions in photolysis coefficients due to the presence of aerosols. Figures 5a-5d compare predictions of ozone to data when aerosols and associated UV absorption were and were not included in model simulations. The inclusion of aerosols not only reduced ozone, but in most cases, it improved ozone predictions, especially of peak mixing ratios.

## 7. Effects of Aerosols on Temperature Profiles

Figures 6a-6n compare predicted (baseline simulation) to observed temperature and dew point profiles at several locations throughout the Los Angeles basin on the afternoons of August 27 and 28, 1987. The figures indicate that the model predicted both parameters consistently at most locations. At Riverside, temperatures were predicted well below 950 mbar on both days and above 800 mbar on the second day. At other pressures, temperatures were underpredicted. Errors in temperature predictions at Riverside resulted in overpredicted inversion base heights on both days, causing excessive vertical dilution of pollutants. Temperature errors aloft at Riverside were not due to soil moisture errors at Riverside since near-surface temperatures were predicted well there. Instead, they were due to errors in elevated heat advection. Observed afternoon winds at Riverside were generally southwesterly below 830 mbar and southeasterly to northeasterly above 830 mbar on August 27-28, 1987. Temperature errors were caused because model winds at Riverside were southeasterly up to 720 mbar; thus, Riverside received cool air from the southeast up to a higher altitude in the model than was observed.

Dew point temperature prediction accuracy decreased between the first and second days of simulation at Burbank and Loyola Marymount. Loyola Marymount is near the coast, and underpredictions of water vapor fluxes from the ocean to atmosphere may have resulted in underpredicted dew point temperatures at this site on the second day. Dew point temperatures were also underpredicted on the second day at Long Beach City College, near the coast, supporting this hypothesis. Since Burbank is affected by coastal air passing over or around the Santa Monica Mountains, errors in ocean water vapor fluxes may have caused errors in dew point temperature at that site on the second day as well.

Figures 7a-7b show vertical profile differences in UV, total solar, and infrared irradiances between the baseline and gas-only simulations at Claremont and Long Beach, respectively, on August 27 at 1130 a.m.. Net irradiance (positive is downward) equals a downward minus an upward irradiance. The figures show that the presence of aerosols enhanced net solar irradiances above the boundary layer at Claremont, slightly decreased them above the boundary layer at Long Beach, and decreased them within the boundary layer at both locations. Aerosols affect net solar irradiance at a given altitude in at least three ways: (1) they backscatter and absorb radiation above the given altitude, reducing the incident downward

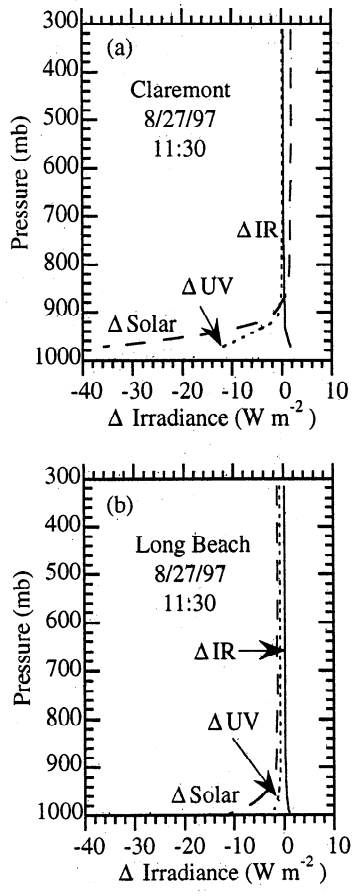


**Figure 7.** Predicted changes in vertical profiles of net (downward minus upward) solar (0.285-2.8 μm), net ultraviolet (0.285-0.385 μm), and net infrared (>2.8 μm) irradiance due to aerosols at (a) Claremont and (b) Long Beach City College at 1130 a.m. on August 27, 1987. A positive value indicates that the presence of aerosols increased the irradiance.

irradiance; (2) they backscatter downward radiation below the given altitude, increasing the upward irradiance and reducing the net downward irradiance at the given altitude; and (3) they absorb visible and UV radiation below the given altitude, reducing the backscattered and ground-reflected upward irradiance and increasing the net downward irradiance at the given altitude. Since aerosols enhanced net downward irradiances above the boundary layer at Claremont, mechanism 3 had a greater impact on the net downward solar fluxes than did mechanisms 1 or 2. At Long Beach, enhanced backscattering by mechanism 2 reduced net downward irradiance above the boundary layer. Within the boundary layer, mechanism 1 dominated at Long Beach and Claremont.

Aerosols decreased net UV irradiances at both locations. Net irradiances decreased more in the boundary layer than aloft. Decreases in new downward net UV irradiance above the boundary layer were most likely due to enhanced backscattering by mechanism 2. Figures 3a-3b show that extinction coefficients due to aerosol scattering in the boundary-layer increased from the visible to UV spectra, supporting this hypothesis for Claremont. Although backscattering aerosols decreased net downward UV irradiances, they increased UV actinic fluxes since backscattering enhances actinic fluxes above the point of backscattering.

Figures 7a-7b indicate that aerosols increased daytime net downward (decreased upward) infrared irradiances at all altitudes, especially in the boundary layer. The decrease in upward irradiance was due to aerosol absorption. As aerosols in a given layer absorbed Earth's infrared irradiance, that irradiance was prevented from backscattering. Figure 8c shows that aerosols also increased net downward infrared irradiance at night, which was expected since aerosols affect infrared radiation in the same way during day and night.

Figures 8a-8c show the effects of aerosols on heating rates and temperatures during a diurnal cycle at Claremont. Figure 8a shows that aerosols increased radiative heating rates and air temperatures in the boundary layer but decreased the ground temperature at 1130 at Claremont. The decrease in ground temperature reduced heat transfer by mechanical and thermal turbulence, reducing near-surface air temperatures. The reduction in near-surface temperatures reached a maximum in the afternoon and was due to turbulence rather than radiative cooling since Figures 8a-8b show that radiative heating rates were positive during the time that air temperatures were decreasing. At night, aerosols increased downward infrared irradiance to the surface, increasing ground temperatures, as is shown in Figure 8c. The increase in ground temperatures increased heat transfer due to mechanical turbulence, increasing boundary layer temperatures. The enhancement in temperatures due to turbulence exceeded the decrease in temperatures due to reduced radiative heating rates in the boundary layer.

Long Beach had a lower aerosol loading in the boundary layer than Claremont. The effects of aerosols on heating rates and temperatures during a diurnal cycle at Long Beach were similar to those at Claremont, except that aerosols caused a smaller net cooling of air temperatures during the day at Long Beach. Boundary layer air temperatures at Long Beach were affected more by the sea breeze than by turbulence.

Figures 8a-8c indicate that during the afternoon, aerosols increased temperatures near the top of the boundary layer but decreased them near the ground. Such changes in temperature increased the stability of the boundary layer. This finding is consistent with similar findings by *Ackerman* [1977] and others, who have used one-dimensional models to examine the effects of aerosols on vertical temperature profiles in an urban area.

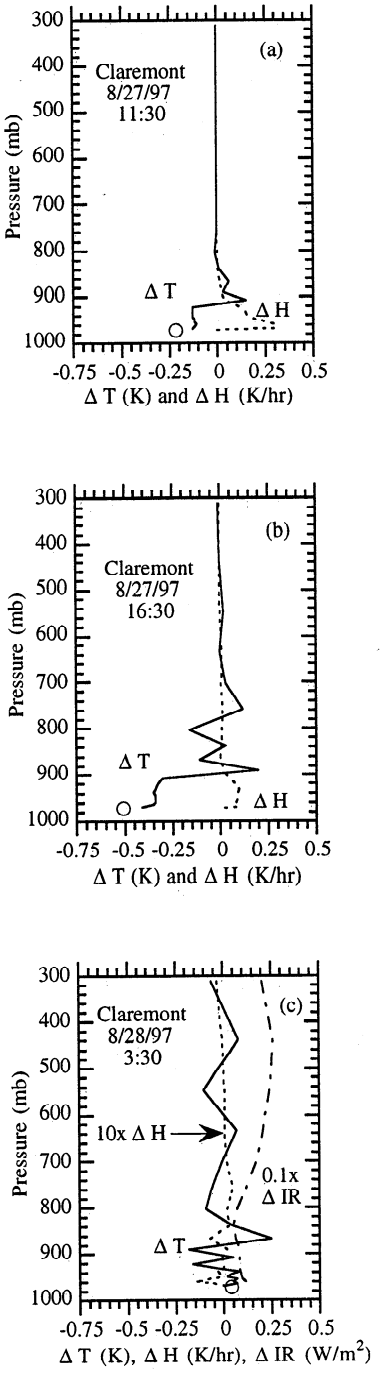


**Figure 8.** Predicted changes in vertical profiles of temperatures and heating rates due to the presence of aerosols at Claremont and Long Beach City College at 1130 and 1630 on August 27, 1987 and 0330 on August 28, 1987. A positive value indicates that the presence of aerosols increased the temperature or heating rate. The circles are ground temperatures. The lowest values on the curve correspond to the midpoint of the bottom model layer.

## 8. Summary

A three-dimensional model was applied to study photolysis rate coefficients and temperatures in the boundary layer and free troposphere above the Los Angeles basin. A baseline simulation that included aerosols and a sensitivity simulation that excluded aerosols were run. Results from both simulations were compared with data for some parameters and to each other for others. The primary conclusions of the study are as follows:

1. In regions of the boundary layer where absorption of UV radiation was strong, aerosols reduced photolysis coefficients of UV-absorbing gases.

2. In regions of the boundary layer where aerosol UV scattering dominated aerosol UV absorption, aerosols enhanced photolysis coefficients of UV-absorbing gases.

3. Since scattering dominated absorption in the visible spectrum, aerosols enhanced photolysis coefficients of gases that photolyzed in the visible spectrum.

4. The presence of scattering and weakly absorbing aerosols above the boundary layer increased photolysis coefficients above the boundary layer for UV- and visible-absorbing gases.

5. Increases in aerosol absorption extinction within the boundary layer reduced spectral actinic fluxes and photolysis rate coefficients above the boundary layer in all cases.

6. Aerosols may have caused up to a 5-8% decrease in near-surface ozone mixing ratios during the Southern California Air Quality Study period.

7. During the day and night, aerosols increased infrared irradiances to the ground. During the day, reductions in surface solar irradiances outweighed increases in infrared irradiances, reducing ground surface temperatures.

8. Because aerosols reduced ground temperatures, they reduced heat transfer to the boundary layer due to mechanical and thermal turbulence, reducing boundary layer temperatures. Aerosols increased radiative heating rates at all altitudes during the day, but cooling due to reduced turbulence outweighed warming due to increased heating rates during the day.

9. During the night, heating rates in the boundary layer decreased but net downward irradiances to the ground increased, increasing ground temperatures. The increase in ground temperatures increased heat transfer to the boundary layer due to mechanical turbulence, increasing boundary layer temperatures.

**Acknowledgments.** A portion of this work was performed on a Cray J-916, provided in part by Cray Research. Cray 90 computer support was also given by the NAS computer facilities in Mountain View, California. This work was supported, in part, by grants from the Environmental Protection Agency under assistance agreement 823186-01-0 and the National Science Foundation under agreements ATM-9504481 and ATM-9614118.

## References

Ackerman, T. P., A model of the effect of aerosols on urban climates with particular applications to the Los Angeles basin, *J. Atmos. Sci.*, *34*, 531-546, 1977.

Atwater, M. A., The radiation budget for polluted layers of the urban environment, *J. Appl. Meteorol.*, *10*, 205-214, 1971a.

Atwater, M. A., Radiative effects of pollutants in the atmospheric boundary layer, *J. Atmos. Sci.*, *28*, 1367-1373, 1971b.

Bergstrom, R., Modelling of the effects of gaseous and particulate pollutants in the urban atmosphere, part I, Thermal structure, *J. Appl. Meteorol.*, *12*, 901-912, 1973a.

Bergstrom, R., Modelling of the effects of gaseous and particulate pollutants in the urban atmosphere, part II, Pollutant dispersion, *J. Appl. Meteorol.*, *12*, 913-918, 1973b.

Bergstrom, R., and R. Viskanta, Prediction of the spectral absorption and extinction coefficients of an urban air pollution aerosol model, *Tellus*, *25*, 468-498, 1973.

Chylek, P., and J. A. Coakley, Jr., Aerosols and climate, *Science*, *183*, 75-77, 1974.

Dean, J. A., *Lange's Handbook of Chemistry*, McGraw-Hill, New York, 1992.

de Arellano, J. V., P. Dynkerke, and M. van Weele, Tethered-balloon measurements of actinic flux in a cloud-capped marine boundary layer, *J. Geophys. Res.*, *99*, 3699-3705, 1994.

Dickerson, R. R., S. Kondragunta, G. Stenchikov, K. L. Civerolo, B. G. Doddridge, and B. N. Holben, The impact of aerosols on solar UV radiation and photochemical smog. *Science*, *278*, 827-830, 1997.

Estournel, C., R. Vehil, D. Guedalia, J. Fontan, and A. Druilhet, Observations and modeling of downward radiative fluxes (solar and infrared) in urban/rural areas, *J. Clim. Appl. Meteorol.*, *22*, 134-142, 1983.

Forster, P. M. de F., Modeling ultraviolet radiation at the earth's surface, part I, The sensitivity of ultraviolet irradiances to atmospheric changes, *J. Appl. Meteor.*, *34*, 2412-2425, 1995.

Foster, V. G., Determination of the refractive index dispersion of liquid nitrobenzene in the visible and ultraviolet, *J. Phys. D. Appl. Phys.*, *25*, 525-529, 1992.

Jacobson, M. Z., Developing, coupling, and applying a gas, aerosol, transport, and radiation model to study urban and regional air pollution. Ph.D. thesis, Univ. of Calif., Los Angeles, 1994.

Jacobson, M. Z., Computation of global photochemistry with SMVGEAR II, *Atmos. Environ.*, *29A*, 2541-2546, 1995.

Jacobson, M. Z., Development and application of a new air pollution modeling system, part II. Aersosol module structure and design, *Atmos. Environ.*, *31*, 131-144, 1997a.

Jacobson, M. Z., Development and application of a new air pollution modeling system, part III, Aerosol-phase simulations, *Atmos. Environ.*, *31*, 587-608, 1997b.

Jacobson, M. Z., Numerical techniques to solve condensational and dissolutional growth equations when growth is coupled to reversible reactions, *Aerosol Sci. Technol.*, *27*, 491-498, 1997c.

Jacobson, M. Z., Improvement of SMVGEAR II on vector and scalar machines through absolute error tolerance control, *Atmos. Environ.*, *32*, in press, 1998a.

Jacobson, M. Z., *Fundamentals of Atmospheric Modeling*, Cambridge Univ. Press, New York, in press, 1998b.

Jacobson, M. Z., R. Lu, R. P. Turco, and O. B. Toon, Development and application of a new air pollution modeling system, part I, Gas-phase simulations, *Atmos. Environ.*, *30B*, 1939-1963, 1996a.

Jacobson, M. Z., A. Tabazadeh, and R. P. Turco, Simulating equilibrium within aerosols and nonequilibrium between gases and aerosols, *J. Geophys. Res.*, *101*, 9079-9091, 1996b.

Kilsby, C. G., A study of aerosol properties and solar radiation during a straw-burning episode using aircraft and satellite measurments, *Q. J. R. Meteorol. Soc.*, *116*, 1173-1192, 1990.

Liou, K.-N., Analytic two-stream and four-stream solutions for radiative transfer, *J. Atmos. Sci.*, *31*, 1473-1475, 1974.

Liou, K.-N., *Radiation and Cloud Processes in the Atmosphere*, Oxford Univ. Press, New York, 1992.

Lu, R., and R. P. Turco, Air pollutant transport in a coastal environment, II, Three-dimensional simulations over Los Angeles basin, *Atmos. Environ.*, *29*, 1499 - 1518, 1995.

Madronich, S., Photodissociation in the atmosphere, 1, Actinic flux and the effects of ground reflections and clouds, *J. Geophys. Res.*, *92*, 9740-9752, 1987.

Mlawer, E. J., S. J. Taubman, P. D. Brown, M. J. Iacono, and S. A. Clough, Radiative transfer for inhomogeneous atmospheres: RRTM, a validated correlated-*k* model for the longwave, *J. Geophys. Res.*, *102*, 16,663-16,682, 1997.

Myrup, L. O., A numerical model of the urban heat island, *J. Appl. Meteor.*, *8*, 908-918, 1969.

Pandis, S. N., R. A. Harley, G. R. Cass, and J. H. Seinfeld, Secondary organic aerosol formation and transport, *Atmos. Environ.*, *26A*, 2269-2282, 1992.

Peterson, J. T., E. C. Flowers, and J. H. Rudisill, Urban-rural solar radiation and atmospheric turbidity measurements in the Los Angeles basin, *J. Appl. Meteorol.*, *17*, 1595-1609, 1978.

Rasool, S. I., and S. H. Schneider, Atmospheric carbon dioxide and aerosols: Effects of large increases on global climate, *Science*, *173*, 138-141, 1971.

Ruggaber, A. R., R. Dlugi, and T. Nakajima, Modelling radiation quantities and photolysis frequencies in the troposphere, *J. Atmos. Chem.*, *18*, 171-210, 1994.

South Coast Air Quality Management District, Draft 1997 air quality management plan for the south coast air basin, Diamond Bar, Calif., 1996.

Tanaka, M., T. Hayasaka, and T. Nakajima, Airborne measurements of optical properties of tropospheric aersools over an urban area, *J. Meteorol. Soc. Jpn.*, *68*, 335-345, 1990.

Toon, O. B., and T. P. Ackerman, Algorithms for the calculation of scattering by stratified spheres, *Appl. Opt.*, *20*, 3657-3660, 1981.

Toon, O. B., C. P. McKay, T. P. Ackerman, and K. Santhanam, Rapid calculation of radiative heating rates and photodissociation rates in inhomogeneous multiple scattering atmospheres, *J. Geophys. Res.*, *94*, 16,287-16,301, 1989.

van Weele, M., and P. G. Duynkerke, Effects of clouds on the photodissociation of $NO_2$: Observation and modelling, *J. Atmos. Chem.*, *16*, 231 - 255, 1993.

Wakimoto, R. M., and J. L. McElroy, Lidar observation of elevated pollution layers over Los Angeles, *J. Clim. Appl. Meteorol.*, *25*, 1583-1599, 1986.

Weare B. C., R. L. Temkin, and F. M. Snell, Aerosols and climate: Some further considerations, *Science*, *186*, 827-828, 1974.

Welch, R., and W. Zdunkowski, A radiation model of the polluted atmospheric boundary layer, *J. Atmos. Sci.*, *33*, 2170-2184, 1976.

Wendisch, M., S. Mertes, A. Ruggaber, and T. Nakajima, Vertical profiles of aerosol and radiation and the influence of a temperature inversion: Measurements and radiative transfer calculations, *J. Appl. Meteorol.*, *35*, 1703-1715, 1996.

Zdunkowski, W. G., and N. D. McQuage, Short-term effects of aerosol on the layer near the ground in a cloudless atmosphere, *Tellus*, *24*, 237-254, 1972.

Zdunkowski, W. G., R. M. Welch, and J. Paegle, One-dimensional numerical simulation of the effects of air pollution on the planetary boundary layer, *J. Atmos. Sci.*, *33*, 2399-2414, 1976.

M. Z. Jacobson, Department of Civil & Environmental Engineering, Terman Engineering Center, Room M-13, Stanford University, Stanford, CA 94305-4020. (E-mail: jacobson@ce.stanford.edu)

**(Received September 4, 1997; revised January 20, 1998; accepted January 21, 1998.)**